

Proceedings of the 2nd Winter Workshop S&SRES'96, Polanica Zdrój 1996

# CROSS RELAXATION AND ENERGY TRANSFER IN $\text{Cs}_2\text{NaSm}_x\text{Eu}_y\text{Y}_{1-x-y}\text{Cl}_6$

T. LUXBACHER, H.P. FRITZER

Institut für Physikalische und Theoretische Chemie  
Technische Universität Graz, 8010 Graz, Austria

AND C.D. FLINT

Laser Laboratory, Department of Chemistry  
Birkbeck College, 29, Gordon Square, London WC1H 0PP, U.K.

Luminescence decay curves have been measured for the  $\text{Sm}^{3+} \ ^4G_{5/2} \rightarrow \ ^6H_{7/2}$  emission in the cubic crystal  $\text{Cs}_2\text{NaSm}_x\text{Eu}_y\text{Y}_{1-x-y}\text{Cl}_6$  ( $x = 0.005$  to  $x = 1$ ,  $y = 0$  to  $y = 0.99$ ) over the temperature range 10 K to 300 K using pulsed laser excitation into the  $\ ^4G_{5/2}$  state of  $\text{Sm}^{3+}$ . The luminescence from the  $\ ^4G_{5/2}$  state of  $\text{Sm}^{3+}$  is strongly quenched by both, cross relaxation to nearest-neighbour  $\text{Sm}^{3+}$  ions and energy transfer to the  $\ ^5D_0$  state of  $\text{Eu}^{3+}$ . We interpret these processes in terms of a recently developed discrete shell model. The dependence of energy transfer from the  $\text{Sm}^{3+}$  donor ion to  $\text{Eu}^{3+}$  acceptor ions on  $y$  is readily studied and modelled. The temperature dependence shows that the cross relaxation occurs mainly by electric dipole vibronic-electric dipole vibronic interaction while in the energy-transfer process magnetic dipole allowed electronic contributions are also involved.

PACS numbers: 33.5.-j, 34.50.Gb, 78.55.Hx

## 1. Introduction

In a recent series of papers [1-6] a discrete shell model has been developed which is particularly suitable for the analysis of cross-relaxation processes between chemically identical ions in systems with high symmetry such as the hexachloroelpasolite crystals  $\text{Cs}_2\text{NaMCl}_6$  ( $M =$  trivalent transition metal or rare-earth ion). In this model there are no free parameters which may be adjusted to describe luminescence decay curves once the cross-relaxation mechanism has been decided. These curves may be calculated directly without any approximations in the mathematical solution of the model once defined. There is *no curve-fitting* involved.

In this contribution the shell model is extended to include energy transfer between dissimilar rare-earth ions in the hexachloroelpasolite lattice. The system  $\text{Cs}_2\text{NaSm}_x\text{Eu}_y\text{Y}_{1-x-y}\text{Cl}_6$  ( $x = 0.005$  to  $x = 1$ ,  $y = 0$  to  $y = 0.99$ ) is chosen for a first comparison between calculation and experiment for these energy-transfer processes. Luminescence decay curves have been measured for the  $\text{Sm}^{3+} \ ^4G_{5/2} \rightarrow \ ^6H_{7/2}$

emission over the temperature range 10 K to 300 K using pulsed laser excitation into the  ${}^4G_{5/2}$  state of  $\text{Sm}^{3+}$ . In this material the luminescence from the  ${}^4G_{5/2}$  state of  $\text{Sm}^{3+}$  is quenched by both, cross relaxation between  $\text{Sm}^{3+}$  ions and energy transfer from  $\text{Sm}^{3+}$  donor ions to  $\text{Eu}^{3+}$  acceptor ions.

This system is particularly suitable for an experimental investigation of the latter energy-transfer process. Firstly, both, the  $\text{Sm}^{3+} {}^4G_{5/2}$  and the  $\text{Eu}^{3+} {}^5D_0$  states have slow intrinsic decay rates over the whole temperature range 10 K to 300 K. Secondly, the energy-transfer rate from  $\text{Sm}^{3+}$  to  $\text{Eu}^{3+}$  is comparable to the intrinsic decay rates of the isolated ions. Thirdly, both, the  $\text{Sm}^{3+} {}^4G_{5/2}$  and the  $\text{Eu}^{3+} {}^5D_0$  state may be separately excited in the region  $17000 \text{ cm}^{-1}$  to  $18000 \text{ cm}^{-1}$  and the emission from these states may be studied with minimum spectral overlap. We focus attention on the material with  $x = 0.01$  over the temperature range 10 K to 300 K. For this concentration of  $\text{Sm}^{3+}$  cross relaxation is weak but not negligible. The cross-relaxation rate has been determined previously from luminescence decay measurements on  $\text{Cs}_2\text{NaSm}_x\text{Y}_{1-x}\text{Cl}_6$  and  $\text{Cs}_2\text{NaSm}_x\text{Gd}_{1-x}\text{Cl}_6$  ( $x = 0.001$  to  $x = 1$ ) [2, 3], and the energy-transfer rate is deduced from the results obtained on  $\text{Cs}_2\text{NaSm}_{0.01}\text{Eu}_{0.99}\text{Cl}_6$ . Results on samples with higher  $\text{Sm}^{3+}$  concentrations are similar to those reported here although the effect of the energy-transfer process between  $\text{Sm}^{3+}$  donor ions and  $\text{Eu}^{3+}$  acceptor ions is smaller especially when  $x > y$ . The dependence of energy transfer from the  $\text{Sm}^{3+}$  donor ion to a single  $\text{Eu}^{3+}$  acceptor ion in the first shell on  $y$  is readily studied and modelled.

## 2. Structural and spectroscopic properties of $\text{Cs}_2\text{NaSm}_x\text{Eu}_y\text{Y}_{1-x-y}\text{Cl}_6$

A diagram of the hexachloroelpasolite lattice has been published previously [1]. The electronic spectra of  $\text{Sm}^{3+}$  and  $\text{Eu}^{3+}$  in  $\text{Cs}_2\text{NaSm}_x\text{Y}_{1-x}\text{Cl}_6$  consist of magnetic-dipole (MD) allowed electronic transitions and electric-dipole allowed vibronic (EDV) transitions [7–13]. The  ${}^6H_{5/2}$  ground state of  $\text{Sm}^{3+}$  is split into two crystal-field components in octahedral symmetry,  $\Gamma_7$  ( $0 \text{ cm}^{-1}$ ) and  $\Gamma_8$  ( $178 \text{ cm}^{-1}$ ). The luminescent electronic state  ${}^4G_{5/2}$  is also split into two components,  $\Gamma_8$  ( $17760 \text{ cm}^{-1}$ ) and  $\Gamma_7$  ( $18105 \text{ cm}^{-1}$ ). The electronic energy levels of  $\text{Eu}^{3+}$  involved in the energy-transfer processes are the  ${}^7F_0$  ground state ( $0 \text{ cm}^{-1}$ ) and the  ${}^7F_1$  state at  $352 \text{ cm}^{-1}$ . The lowest lying luminescent state is  ${}^5D_0$  at  $17220 \text{ cm}^{-1}$ .

The odd parity vibrational modes  $\nu_6$ ,  $\nu_4$ , and  $\nu_3$  of the  $[\text{LnCl}_6]^{3-}$  ion ( $\text{Ln} = \text{Sm}, \text{Eu}$ ) are about  $80 \text{ cm}^{-1}$  ( $\nu_6$ ),  $100 \text{ cm}^{-1}$  ( $\nu_4$ ), and  $250 \text{ cm}^{-1}$  ( $\nu_3$ ) [8, 13] and contribute to the energy-transfer processes. Lattice vibrations are found at  $40 \text{ cm}^{-1}$  and  $180 \text{ cm}^{-1}$ . The cross-relaxation processes involving the  ${}^4G_{5/2} \rightarrow {}^6F_J$  ( $J = 7/2, 9/2, 11/2$ ) relaxation at the donor and the  ${}^6H_{5/2} \rightarrow {}^6F_J$  ( $J = 5/2, 9/2, 11/2$ ) transitions at the acceptor have been described in detail previously [2] and are shown in Fig. 1 as pairs of transitions *A*, *B*, and *C*. Energy transfer occurs to the  $\text{Eu}^{3+} {}^5D_0$  level. At high temperatures the  $({}^4G_{5/2})\Gamma_7 \rightarrow ({}^6H_{7/2})\Gamma_7, \Gamma_8$  donor transitions are almost resonant with the  $\text{Eu}^{3+} ({}^7F_1)\Gamma_4 \rightarrow ({}^5D_0)\Gamma_1$  MD electronic transition (transitions *E* in Fig. 1) [7, 10]. At low temperatures the main contribution to the energy-transfer process involves the  ${}^4G_{5/2} \rightarrow {}^6H_{5/2}$  transitions at the  $\text{Sm}^{3+}$  donor ion and the  ${}^7F_0 \rightarrow {}^5D_0$  EDV transition at the  $\text{Eu}^{3+}$  acceptor ion (transitions *D* in Fig. 1).

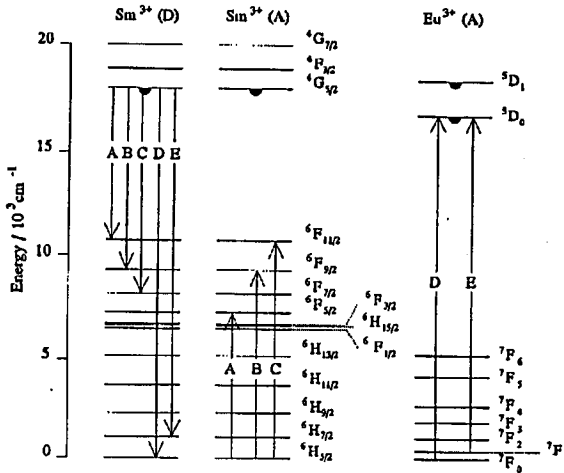


Fig. 1. Relevant energy levels and transitions involved in the cross-relaxation and energy-transfer processes in  $\text{Cs}_2\text{NaSm}_x\text{Eu}_y\text{Y}_{1-x-y}\text{Cl}_6$ . The letters indicate pairs of near resonant transitions.

### 3. Experimental

Single crystals of  $\text{Cs}_2\text{NaSm}_x\text{Eu}_y\text{Y}_{1-x-y}\text{Cl}_6$  were grown by the Bridgman technique as described previously [2]. Luminescence decay measurements were carried out as described in Ref. [2] using a Spectron doubled Nd:YAG laser pumping a Spectron dye laser with Rhodamin 6G dissolved in ethanole as the laser dye. The decay of the  $(^4\text{G}_{5/2})\Gamma_8 \rightarrow (^6\text{H}_{7/2})\Gamma_8, \Gamma_7$  emission of  $\text{Sm}^{3+}$  was observed at  $16525 \pm 20 \text{ cm}^{-1}$  over a temperature range of 10 K to 300 K after excitation into the MD allowed  $(^6\text{H}_{5/2})\Gamma_7 \rightarrow (^4\text{G}_{5/2})\Gamma_8$  transition at  $17760 \text{ cm}^{-1}$ .

### 4. The shell model for energy transfer

Our shell model assumes Förster-Dexter multipole-multipole interactions between statistically distributed donor and acceptor ions, where the rate of resonant energy transfer from a donor ion D to an acceptor ion A may be written [14, 15] as

$$k^{\text{ET}} = \frac{2\pi}{\hbar} \sum_{\substack{d, d' \\ a, a'}} p_{d'} p_a |\langle da' | \hat{H}_{\text{DA}} | d'a \rangle|^2 \int g_{d'd}(E) g_{a'a'}(E) dE, \quad (1)$$

$p_{d'}$  and  $p_a$  give the normalized populations of donor state  $d'$  and acceptor state  $a$ , and the overlap integral contains normalized lineshape functions. Within the shell model the luminescence decay curves following a  $\delta$ -function excitation pulse take the form

$$I(t) = I(0) \exp(-k_0 t) \prod_n^{\text{shells}} \sum_{r_n}^{N_n} \sum_{q_n}^{N_n - r_n} O_{r_n, q_n}^{N_n} (x, y) \times \exp \left[ -G_n^s (r_n k^{\text{CR}} + q_n k^{\text{ET}}) \left( \frac{R_1}{R_n} \right)^s t \right]. \quad (2)$$

The model assumes that excitation intensities are low and that back transfer of excitation energy and migration among the donors are negligible.  $x$  is the mole fraction of the rare-earth ion,  $R_n$  is the distance between the donor ion and an acceptor in the  $n$ -th shell,  $k_0$  is the intrinsic decay rate involving radiative and non-radiative single-ion processes,  $k^{\text{CR}}$  is the cross-relaxation rate to a single acceptor in the first shell, and  $k^{\text{ET}}$  is the energy-transfer rate between dissimilar ions, where the acceptor occupies a nearest-neighbour lattice site.  $s = 6, 8, \text{ or } 10$  for EDV-EDV and MD-MD, EDV-electric quadrupole (EQ), and EQ-EQ interactions, respectively. In the present system there is no evidence for multipole-multipole interactions involving  $s > 6$ . The angular dependence of this dipole-dipole coupling,  $G_n^6$ , is then independent of the value of  $n$  [1] and is included in the definitions of  $k^{\text{CR}}$  and  $k^{\text{ET}}$ . The occupancy factor  $O_{r_n, q_n}^{N_n}(x, y)$  in this system is the statistical probability of there being  $r_n$  ions chemically identical to the donor and  $q_n$  ions of the chemically different acceptor in the  $n$ -th shell which has a capacity to contain  $N_n$  acceptors and is readily computed from the equation

$$O_{r_n, q_n}^{N_n}(x, y) = \frac{N_n!}{(N_n - r_n - q_n)! r_n! q_n!} x^{r_n} y^{q_n} (1 - x - y)^{N_n - r_n - q_n}. \quad (3)$$

For the elpasolite lattice, more than 94% of the energy-transfer processes are described by using the first three shells [3]. We therefore truncate the expansion in Eq. (2) at this point. All values of the occupancy factor have been included. This represents a summation over about  $8.3 \times 10^5$  acceptor distributions.

## 5. Results and discussion

### 5.1. $\text{Cs}_2\text{NaSm}_x\text{Y}_{1-x}\text{Cl}_6$

Luminescence decay of the  ${}^4\text{G}_{5/2} \rightarrow {}^6\text{H}_{7/2}$  emission of an isolated  $\text{Sm}^{3+}$  ion has been measured in  $\text{Cs}_2\text{NaSm}_{0.005}\text{Y}_{0.995}\text{Cl}_6$  over the temperature range 10 K to 300 K [2, 3]. The decay curves are exactly exponential over 10 half-lives and correspond to decay constants of  $58 \text{ s}^{-1}$  at 10 K increasing to  $107 \text{ s}^{-1}$  at 300 K. The variation in  $k_0$  with temperature normalized to its value at 10 K is shown as curve *a* in Fig. 2. The temperature dependence of  $k_0$  is entirely consistent with the relaxation mechanism being due to the sum of MD allowed electronic transitions and EDV transitions following the coth law [3, 16].

As the concentration of  $\text{Sm}^{3+}$  is increased, cross relaxation involving the  ${}^4\text{G}_{5/2} \rightarrow {}^6\text{F}_J$  ( $J = 7/2, 9/2, 11/2$ ) transitions at the donor and the  ${}^6\text{H}_{5/2} \rightarrow {}^6\text{F}_J$  ( $J = 5/2, 9/2, 11/2$ ) transitions at the acceptor becomes increasingly important (e.g., pairs of transitions *A*, *B*, and *C* in Fig. 1). The cross-relaxation rate may be determined from the exponential decay of luminescence from the  ${}^4\text{G}_{5/2}$  state of  $\text{Sm}^{3+}$  in  $\text{Cs}_2\text{NaSmCl}_6$  since the decay constant of the  $x = 1$  crystal equals

$$k_0 + \left[ \sum_{n=1}^3 N_n \left( \frac{R_1}{R_n} \right)^6 \right] k^{\text{CR}} = k_0 + (12 + 6/8 + 24/27) k^{\text{CR}} = k_0 + 14.4 k^{\text{CR}} \quad (4)$$

for three-shell dipole-dipole interaction [1, 3]. The measured exponential decay constant for  $x = 1$  at 10 K is  $11600 \text{ s}^{-1}$  corresponding to  $k^{\text{CR}}(\text{DD}) = 850 \text{ s}^{-1}$

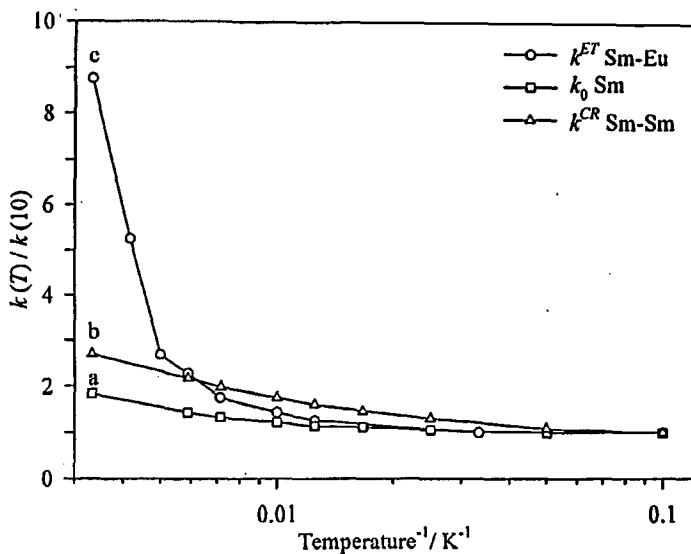


Fig. 2. Temperature dependence of the intrinsic decay (a), cross-relaxation (b), and energy-transfer rates (c) of  $\text{Sm}^{3+}$  normalized to the values  $k_0 = 58 \text{ s}^{-1}$ ,  $k^{\text{CR}}(\text{DD}) = 850 \text{ s}^{-1}$ , and  $k^{\text{ET}}(\text{DD}) = 5.7 \text{ s}^{-1}$  at 10 K.

increasing by a factor of 2.7 at 300 K. The temperature dependence of this rate normalized to its value at 10 K is shown as curve *b* in Fig. 2. Again this rate is entirely consistent with an EDV-EDV cross-relaxation mechanism. The stronger temperature dependence of  $k^{\text{CR}}$  is due to this quantity being proportional to the product of two vibronic mechanisms and the minimum contribution of MD processes. The decay curve for  $x = 0.01$  is identical to that for  $x = 0.005$  at times greater than  $2.5 \times 10^{-3} \text{ s}$ . At short times there is a small faster component consistent with the value of  $O_1^{12}(0.01) = 0.1$  [2] and  $k^{\text{CR}}$  taking the values of curve *b* in Fig. 2.

### 5.2. $\text{Cs}_2\text{NaSm}_{0.01}\text{Eu}_y\text{Y}_{0.99-y}\text{Cl}_6$

Introduction of  $\text{Eu}^{3+}$  into the  $x = 0.01$  crystal results in an increase in the rate of relaxation from the  ${}^4G_{5/2}$  state of  $\text{Sm}^{3+}$  due to energy transfer to the  ${}^5D_0$  state of  $\text{Eu}^{3+}$ . Figure 3 shows luminescence decay curves from the  ${}^4G_{5/2}$  state of  $\text{Sm}^{3+}$  in  $\text{Cs}_2\text{NaSm}_{0.01}\text{Eu}_y\text{Y}_{0.99-y}\text{Cl}_6$  for  $0 \leq y \leq 0.99$  at 80 K. The decay curves for  $y \leq 0.1$  and  $y = 0.99$  are essentially exponential at times  $> 2.5 \times 10^{-3} \text{ s}$ . At intermediate concentrations the long time decay curves deviate significantly from pure exponential behaviour but are exactly described by Eq. (2). In Fig. 3 the *a priori* calculated decay curves for  $\text{Cs}_2\text{NaSm}_{0.01}\text{Eu}_y\text{Y}_{0.99-y}\text{Cl}_6$  assuming  $s = 6$  in Eq. (2) are superimposed on the measured curves. We emphasize that in Fig. 3 *no curve-fitting* is involved. We have included only the first three shells in our model using the exponential decay constants  $k_0 = 66 \text{ s}^{-1}$  and  $k^{\text{CR}}(\text{DD}) = 1350 \text{ s}^{-1}$  from our previous measurements on  $\text{Cs}_2\text{NaSm}_{0.005}\text{Y}_{0.995}\text{Cl}_6$  and  $\text{Cs}_2\text{NaSmCl}_6$  at

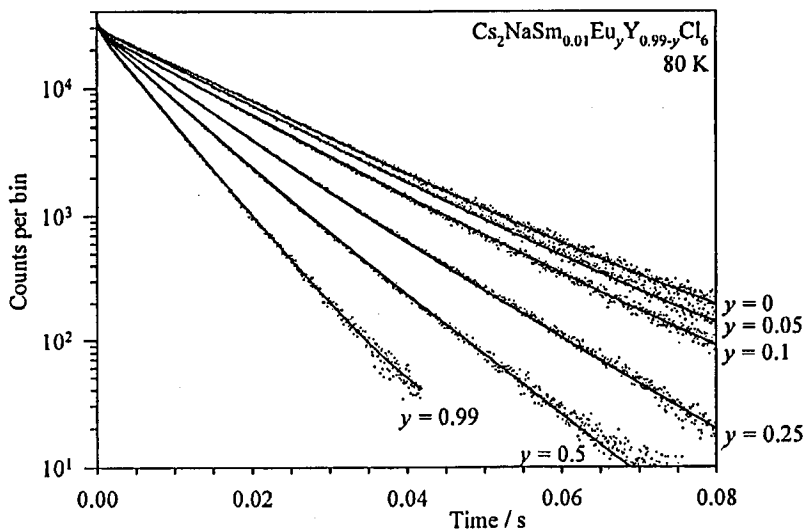


Fig. 3. Dependence of the luminescence decay from the  ${}^4G_{5/2}$  state of  $\text{Sm}^{3+}$  in  $\text{Cs}_2\text{NaSm}_{0.01}\text{Eu}_y\text{Y}_{0.99-y}\text{Cl}_6$  on  $y$ . Note that the solid lines are calculated *a priori* using  $k_0 = 66 \text{ s}^{-1}$ ,  $k^{\text{CR}}(\text{DD}) = 1350 \text{ s}^{-1}$ , and  $k^{\text{ET}}(\text{DD}) = 7.2 \text{ s}^{-1}$ .

80 K, respectively [2, 3]. For contributions from  $n > 1$  shells, parameters reflecting effects like screening of electrostatic interaction by the crystal lattice have been introduced to describe the measured curves more accurately. We note that due to the low  $\text{Sm}^{3+}$  concentration ( $x = 0.01$ ) the contributions from 2-nd and 3-rd shells are very small such that the absence or presence of electrostatic shielding by the surrounding lattice ions cannot be determined. The rate  $k^{\text{ET}}(\text{DD}) = 7.5 \text{ s}^{-1}$  for energy transfer from  $\text{Sm}^{3+}$  donors to  $\text{Eu}^{3+}$  acceptors has been determined from the measured luminescence decay curve of  $\text{Cs}_2\text{NaSm}_{0.01}\text{Eu}_{0.99}\text{Cl}_6$  at 80 K. This value has been used to calculate the decay curves for all other  $\text{Eu}^{3+}$  concentrations.

The behaviour at all other temperatures is similar with the energy-transfer rate increasing much more rapidly than either  $k_0$  or  $k^{\text{CR}}$  at temperatures greater than 80 K. The variation of  $k^{\text{ET}}$  with temperature normalized to its value at 10 K is shown as curve *c* in Fig. 2. The temperature dependence of the energy-transfer rate indicates that two different mechanisms are involved.

At low temperatures the most probable mechanism for energy transfer from  $\text{Sm}^{3+}$  donors to  $\text{Eu}^{3+}$  acceptors in the system  $\text{Cs}_2\text{NaSm}_x\text{Eu}_y\text{Y}_{1-x-y}\text{Cl}_6$  involves the  $({}^4G_{5/2})\Gamma_8 \rightarrow ({}^6H_{5/2})\Gamma_8 + \nu_{\text{vib}}$  EDV transition at the donor and the  $({}^7F_0)\Gamma_1 \rightarrow ({}^5D_0)\Gamma_1 + \nu'_{\text{vib}}$  EDV transition at the acceptor (transitions *D* in Fig. 1). The energy mismatch  $\nu_{\text{vib}} + \nu'_{\text{vib}}$  is  $395 \text{ cm}^{-1}$  and can be bridged by coupling to the odd parity vibrational modes of the  $[\text{LnCl}_6]^{3-}$  ion, e.g., annihilation of  $\nu_3$  at the  $\text{Sm}^{3+}$  donor transition and creation of  $\nu_{\text{lattice}}$  at the  $\text{Eu}^{3+}$  acceptor transition.

At temperatures above 80 K a resonant pathway becomes important involving the  $({}^4G_{5/2})\Gamma_7 \rightarrow ({}^6H_{7/2})\Gamma_7, \Gamma_8$  transitions at  $16866 \text{ cm}^{-1}$  and  $16879 \text{ cm}^{-1}$  at the donor and the  $({}^7F_1)\Gamma_4 \rightarrow ({}^5D_0)\Gamma_1$  transition at  $16857 \text{ cm}^{-1}$  at the acceptor

(transitions  $E$  in Fig. 1), where both transitions are of MD allowed electronic origin [9, 17]. The temperature dependence of this resonant energy-transfer process is introduced by the Boltzmann factors and the overlap integral in Eq. (1). The normalized lineshape functions depend on the position and width of the donor emission and acceptor absorption lines which show a  $T^4$  and  $T^7$  dependence, respectively [18].

## 6. Conclusions

In this contribution we have discussed the dependence of the time evolution of donor luminescence from the  ${}^4G_{5/2}$  state of  $\text{Sm}^{3+}$  on the  $\text{Eu}^{3+}$  concentration in  $\text{Cs}_2\text{NaSm}_{0.01}\text{Eu}_y\text{Y}_{0.99-y}\text{Cl}_6$  in terms of a discrete shell model.

The temperature dependence of the energy-transfer rate  $k^{\text{ET}}$  from a  $\text{Sm}^{3+}$  donor ion to a single  $\text{Eu}^{3+}$  acceptor ion in the  $n = 1$  shell can be explained by assuming two different mechanisms. At low temperature phonon-assisted energy transfer is dominant while resonant transfer involving the magnetic dipole allowed  ${}^7F_1 \rightarrow {}^5D_0$  transition of  $\text{Eu}^{3+}$  becomes important as the temperature is increased.

The energy-transfer rate  $k^{\text{ET}}$  is small compared to the intrinsic decay rate  $k_0$ . Therefore, effects like selective screening of multipolar interaction between donor and  $n > 1$  acceptor ions which give rise to discrepancies between calculated and experimental decay curves in the cross-relaxation regime, are not observable for energy transfer from  $\text{Sm}^{3+}$  donor ions to  $\text{Eu}^{3+}$  acceptors.

## Acknowledgments

This work has been supported in part under the collaborative ARC scheme of the British Council and the Bundesministerium für Wissenschaft und Forschung.

## References

- [1] S.O. Vasquez, C.D. Flint, *Chem. Phys. Lett.* **238**, 378 (1995).
- [2] T. Luxbacher, H.P. Fritzer, R. Sabry-Grant, C.D. Flint, *Chem. Phys. Lett.* **241**, 103 (1995).
- [3] T. Luxbacher, H.P. Fritzer, C.D. Flint, *J. Phys., Condens. Matter* **7**, 9683 (1995).
- [4] S.O. Vasquez, C.D. Flint, *J. Appl. Spectrosc.* **62**, 213 (1995).
- [5] T. Luxbacher, K. Gatterer, H.P. Fritzer, C.D. Flint, *J. Appl. Spectrosc.* **62**, 27 (1995).
- [6] R. Sabry-Grant, C.D. Flint, *J. Appl. Spectrosc.* **62**, 155 (1995).
- [7] D.R. Foster, F.S. Richardson, R.W. Schwartz, *J. Chem. Phys.* **82**, 618 (1985).
- [8] A.K. Banerjee, R.W. Schwartz, *Chem. Phys.* **58**, 255 (1981).
- [9] P.A. Tanner, *Chem. Phys. Lett.* **155**, 59 (1989).
- [10] M. Bettinelli, C.D. Flint, *Chem. Phys. Lett.* **167**, 45 (1990).
- [11] R.W. Schwartz, *Mol. Phys.* **30**, 81 (1975).
- [12] O.A. Serra, L.C. Thompson, *Inorg. Chem.* **15**, 504 (1976).
- [13] C.D. Flint, F.L. Stewart-Darling, *Mol. Phys.* **44**, 61 (1981).
- [14] T. Förster, *Ann. Phys.* **2**, 55 (1948).

- [15] D.L. Dexter, *J. Chem. Phys.* **21**, 836 (1953).
- [16] A.D. Liehr, C.J. Ballhausen, *Phys. Rev.* **106**, 1161 (1957).
- [17] M. Bettinelli, C.D. Flint, *J. Phys., Condens. Matter* **3**, 4433 (1991).
- [18] D.E. McCumber, M.D. Sturge, *J. Appl. Phys.* **34**, 1682 (1963).